Numerical study of the Kerr solution in rotating coordinates

S. Bai, G. Izquierdo,* and C. Klein†
Institut de Mathématiques de Bourgogne, Université de Bourgogne,
9 avenue Alain Savary, 21078 Dijon Cedex, France
(Dated: February 23, 2016)

The Kerr solution in coordinates corotating with the horizon is studied as a testbed for a spacetime with a helical Killing vector in the Ernst picture. The solution is numerically constructed by solving the Ernst equation with a spectral method and a Newton iteration. We discuss convergence of the iteration for several initial iterates and different values of the Kerr parameters.

PACS numbers: 04.25.dg

arXiv:1602.06400v1 [gr-qc] 20 Feb 2016

I. INTRODUCTION

Binary black holes in the latest stage before an eventual merger were generally seen as the most promising sources of gravitational waves to be detected with current ground based interferometers, and this has been done just recently in [1]. Solutions to the Einstein equations for such configurations can only be found numerically with current knowledge, and considerable progress has been made in the last decade in this context, see for instance [2] for a recent review of the field. It is generally assumed that there is a quasi-stationary phase of such a system before the inspiral where the change of the radius of the binary orbit due to emitted gravitational radiation is relatively small during one complete turn. Detweiler [3–5] suggested to approximate this quasi-circular phase by a system where the outgoing radiation is exactly compensated by incoming radiation. This approximation had been previously used for binary charges of opposite sign in Maxwell theory by Schönberg [6] and Schild [7].

In a general relativistic context, this approximation corresponds to the presence of a helical Killing vector. For the phase of quasicircular orbits of binary systems, this concept has proven very fruitful in numerical computations, see for instance [8–20] and references therein. Interesting numerical concepts have been developed in these references, see also [21–23]. Helical Killing vectors have also proven to be useful in post-Newtonian calculations [24–26].

Spacetimes with a helical Killing vector are also interesting from a mathematical point of view. If such a Killing vector is global, the spacetime cannot have a regular null infinity, see [27, 28]. Loosely speaking the reason for this is that the incoming radiation needed to compensate the outgoing radiation in a nonlinear theory does not allow for a regular null infinity. As discussed for instance in [29] in a formal expansion, invariants of the Weyl tensor should have an oscillation point at null infinity. A characteristic feature of a helical Killing vector is the change of sign of his norm at the *light cylinder*, a surface of cylindrical topology. This can be understood most easily in Minkowski spacetime where $\xi = \partial_t + \Omega\partial_\phi$ with $\Omega = const$ is a helical Killing vector in standard cylindrical coordinates, i.e., one just passes into a rotating frame. The norm of the Killing vector is in this case $f = 1 - \Omega^2\rho^2$, and the light cylinder corresponds to $\rho_c = 1/\Omega$. In the rotating frame, the helically reduced flat d'Alembert operator reads

$$\mathcal{L} := \partial_{\rho\rho} + \frac{1}{\rho}\partial_\rho + \partial_{zz} + (1 - \Omega^2\rho^2)\frac{1}{\rho^2}\partial_{\phi\phi}. \qquad (1)$$

Inside the light cylinder the operator is elliptic, outside hyperbolic. Such spacetimes with signature changes appear also in other relativistic contexts, see [30]. Equations of mixed type are often a consequence of symmetry reductions as here where the norm of the Killing vector changes sign, see [31]. Operators of the type (1) belong to the symmetric positive equations discussed by [32] and [33]. Questions of existence and uniqueness of solutions for equations in the context of helical Killing vectors were discussed in [34, 35], and in a general context in [36–38]. Concrete examples for helical Killing vectors in various settings were discussed in [39–41].

In [29] the existence of a helical Killing vector in a spacetime was to used to factorize the metric with respect to the symmetry in a projection formalism first applied by Ehlers [42], see also [43, 44]. In this case the Einstein equations can be written in the form of a complex Ernst equation [45] which replaces the constraint equations in a standard $3+1$ decomposition. The remaining Einstein equations describe a model of 3-dimensional gravity coupled to a sigma model, see [46, 47].

This rather elegant form of the equations has the disadvantage that the Killing horizons and the light cylinder are singularities of the equations. Thus it is not clear whether they are useful for numerical computations. To address this question, we study in this paper for a simple test case whether the numerical issues in this formalism can be surmounted. To this end we consider the exact Kerr solution in a frame corotating with the horizon. In this frame, the norm of the helical Killing vector vanishes at the horizon and at the light cylinder. The 3-metric is prescribed, thus the only equation to be solved is the

*Current address: Facultad de Ciencias, Universidad Autónoma del Estado de México, Toluca 5000, Instituto literario 100, Edo. Mex., México.
†Electronic address: christian.klein@u-bourgogne.fr

Ernst equation.

To solve the latter, we use a finite computational domain between the horizon and an outer radius where the exact Kerr solution is imposed as boundary values. The equations are solved with a spectral method and a Newton iteration. The Komar integral is imposed in the iteration to address non-uniqueness issues. It is shown that the iteration converges rapidly unless the light cylinder is close to the computational boundary. In this case the iteration is amended with an Armijo scheme [48].

The paper is organized is follows: In secction 2, we briefly review the projection formalism and the Ernst equation. In section 3 we give the Ernst potential for the Kerr solution in coordinates corotating with the horizon. In the same coordinates, the Ernst equation is formulated in section 4. The used numerical approaches for the paper are presented in section 5. In section 6 we discuss the convergence of the scheme for various initial iterates and parameters of the Kerr solution. We add some concluding remarks in section 7.

II. QUOTIENT SPACE METRICS AND ERNST EQUATIONS

In this section we briefly summarize the approach to binary black hole spacetimes with a helical Killing vector of [29] based on quotient space metrics first used in [42] (see also [43]) in the form of [44] and Ernst equations. The existence of a Killing vector ξ, in adapted coordinates $\xi = \partial_t$ where t is not necessarily a timelike coordinate, can be used to establish a simplified version of the field equations by dividing out the group action. The norm of the Killing vector will be denoted by f.

In this approach, the metric is written in the form

$$ds^2 = -f(dt + k_a dx^a)(dt + k_b dx^b) + \frac{1}{f} h_{ab} dx^a dx^b; \quad (2)$$

latin indices always take the values $1, 2, 3$ corresponding to the spatial coordinate. Note that this decomposition is not defined at the fixed points of the group action, i.e. the zeros of f. The Einstein equations will be singular at the set of zeros of f which is also a problem for a numerical treatment. Note that this will not be the case in a standard 3+1 decomposition of spacetime. But as will be shown in this paper, the related numerical issues can be controlled, and thus the simplicity of the quotient space approach with respect to a standard $3+1$ decomposition can be also used in a numerical approach.

The Einstein equations in vacuum can be put into the form of the complex Ernst equation

$$f D_a D^a \mathcal{E} = D_a \mathcal{E} D^a \mathcal{E}. \quad (3)$$

Here the complex Ernst potential is given by $\mathcal{E} = f + ib$ [45], where D_a denotes the covariant derivative with respect to h_{ab}, where the twist potential b is defined via (ϵ^{abc} is the tensor density with $\epsilon^{123} = 1/\sqrt{h}$)

$$k^{ab} = \frac{1}{f^2} \epsilon^{abc} b_{,c}, \quad (4)$$

where h is the determinant of h_{ab}, where $k_{ab} = k_{b,a} - k_{a,b}$, and where all indices are raised and lowered with h_{ab}.

The equations for the metric h_{ab} can be written in the form

$$R_{ab} = \frac{1}{2f^2} \Re(\mathcal{E}_{,a} \bar{\mathcal{E}}_{,b}), \quad (5)$$

where R_{ab} is the three-dimensional Ricci tensor corresponding to h_{ab}. It is obvious that zeros of the norm of the Killing vector are singular points of the equations.

Thus the equations for the metric function h_{ab} are the three dimensional Einstein equations with some energy momentum tensor which is a so-called sigma model, see the discussion in [29] and references therein. Thus one can introduce a 2+1 decomposition of the quotient space, preferably a foliation with respect to some coordinate r in which the horizons of the black holes are constant r surfaces. It is well known that the 6 equations (5) split in this case into 3 'evolution equations' containing second order derivatives with respect to this coordinate r, and 3 'constraints' containing at most first derivatives with respect to r, see [29] for the helical case. If both of these pairs of equations are satisfied on the horizons, it will be sufficient to solve one of them in the space in between.

Thus the problem for binary black holes with a helical Killing vector is reduced to solving the Ernst equation (3) and 3 of the equations (5) which are of first order in the derivatives with respect to this coordinate r (which need not be related to spherical coordinates). All these equations are singular at the zeros of the norm f of the Killing vector, the horizons and the light cylinder. In order to solve these equations numerically, one is faced with a singular boundary value problem with a singular light cylinder the position and form of which is not known a priori. In particular it has cylindrical topology and can thus not be an $r = const$ surface.

As a test problem for these issues which is analytically known, we will study in this paper the Kerr black hole in a frame corotating with the horizon. The Kerr spacetime is stationary and axisymmetric, and both Killing vectors ∂_t and ∂_ϕ in an asymptotically non rotating coordinate system are commuting. This means that $\xi = \partial_t + \Omega \partial_\phi$ is also a Killing vector for arbitrary constant value of Ω. We will consider the value of Ω for which the norm of ξ vanishes at the horizon of the Kerr black hole. In the stationary axisymmetric case, the metric h_{ab} can be chosen to be diagonal with a single unknown function, see for instance [47, 49]. This function can be obtained via a line integration in closed form. With this function given, the task is reduced to solve the Ernst equation. The vector k_a can be chosen to have just a ϕ compoment which will be denoted by a. The model has a vanishing f at the horizon for the Killing vector ∂_t, a light cylinder and the asymptotically rotating coordinate system. Thus

a numerical approach to reproduce the Kerr solution in this setting could be possibly extended to the case of binary black hole spacetimes with a helical Killing vector. We treat this problem on a finite computational domain bounded on one side by the black hole horizon and on the other by the exact Kerr solution which we impose for simplicity as a boundary condition. In the general case one would impose instead boundary values inferred from the asymptotic behavior of the solution, for instance a solution to the linearized Einstein equations as discussed in [29].

Note that we only consider the Ernst equation here since it already has all relevant features we want to test for the binary case with a helical Killing vector. The metric h is given for a known Ernst potential via a first order equation. In the iterative approach to solve the equations we are applying here, this means that in each step of the iteration the metric h will be obtained via a quadrature. Thus to test the approach for the Kerr solution, it is sufficient to give the exact metric h and to solve merely the Ernst equation.

III. KERR SOLUTION IN ROTATING COORDINATES

In this section we give the Kerr solution in the Ernst formalism in coordinates corotating with the horizon. In *Boyer-Lindquist coordinates* r, θ, ϕ, the Kerr solution for a single black hole with mass m and angular momentum $J = m^2 \sin\varphi$ takes the form (see for instance [49] and references therein)

$$\begin{aligned} f &= \frac{r^2 - 2mr + m^2 \sin^2\varphi\cos^2\vartheta}{r^2 + m^2\sin^2\varphi\cos^2\vartheta}, \\ b &= -\frac{2m^2\sin\varphi\cos\vartheta}{r^2 + m^2\sin^2\varphi\cos^2\vartheta} \end{aligned} \tag{6}$$

and

$$a = \frac{2m^2\sin\varphi r\sin^2\vartheta}{r^2 - 2mr + m^2\sin^2\varphi\cos^2\vartheta}. \tag{7}$$

The parameter φ varies between 0, the Schwarzschild solution, and $\pi/2$, the extreme Kerr solution. The metric h reads

$$\begin{aligned} h_{rr} &= = \frac{r^2 - 2mr + m^2\sin^2\varphi\cos^2\vartheta}{(r-R)\left(r - 2m\sin^2\frac{\varphi}{2}\right)}, \\ h_{\vartheta\vartheta} &= r^2 - 2mr + m^2\sin^2\varphi\cos^2\vartheta, \\ h_{\phi\phi} &= (r-R)\left(r - 2m\sin^2\frac{\varphi}{2}\right)\sin^2\vartheta. \end{aligned} \tag{8}$$

The horizon is located in these coordinates at $R = 2m\cos^2\frac{\varphi}{2}$. At the horizon we have for (7)

$$a = -1/\Omega_{BH} = -2m\cot\frac{\varphi}{2} \tag{9}$$

where Ω_{BH} is the angular velocity that can be attributed to the horizon with respect to an observer at infinity. The metric function $h_{\phi\phi}$ vanishes at the horizon.

The solution is here given in an asymptotically non rotating frame. Using a transformation of the form $\phi' = \phi + \Omega t$, we get

$$\begin{aligned} g'_{00} &= g_{00} + 2\Omega g_{03} + \Omega^2 g_{33}, \\ g'_{03} &= g_{03} + \Omega g_{33}. \end{aligned} \tag{10}$$

For f and a this implies

$$f' = f(1+\Omega a)^2 - \Omega^2 h_{\phi\phi}/f, \quad a'f' = af(1+\Omega a) - \Omega h_{\phi\phi}/f. \tag{11}$$

In corotating coordinates ($\Omega = \Omega_{BH}$), we have for (7)

$$1 + \Omega a = \frac{(r-R)(r - 2m\sin^2\frac{\varphi}{2}\cos^2\vartheta)}{r^2 - 2mr + m^2\sin^2\varphi\cos^2\vartheta}. \tag{12}$$

Thus f' vanishes in coordinates corotating with the horizon as $r - R$ for $r \to R$ because of the linear term in $h_{\phi\phi}$. The term $(1 + \Omega a)^2$ is quadratic in $r - R$.

For the Kerr solution in Boyer-Lindquist coordinates, eq. (11) implies with $\tilde{r} = r/R$

$$\begin{aligned} f' = \frac{\tilde{r} - 1}{\tilde{r}^2 + \tan^2\frac{\varphi}{2}\cos^2\vartheta} \Big\{ &-\sin^2\frac{\varphi}{2}\cos^2\frac{\varphi}{2}\sin^2\vartheta(\tilde{r}^3 + \tilde{r}^2) \\ &+ \left(1 - \sin^2\frac{\varphi}{2}\sin^2\vartheta - \sin^4\frac{\varphi}{2}\sin^2\vartheta\cos^2\vartheta\right)\tilde{r} \\ &- \tan^2\frac{\varphi}{2}\cos^2\vartheta + \tan^2\frac{\varphi}{2}\sin^4\frac{\varphi}{2}\sin^2\vartheta\cos^2\vartheta \Big\} \end{aligned} \tag{13}$$

and

$$\begin{aligned} a'f' = \frac{2m\tan\frac{\varphi}{2}\sin^2\vartheta(\tilde{r} - 1)}{\tilde{r}^2 + \tan^2\frac{\varphi}{2}\cos^2\vartheta} \Big\{ &-\cos^4\frac{\varphi}{2}(\tilde{r}^3 + \tilde{r}^2) \\ &- \cos^2\frac{\varphi}{2}\left(1 + \sin^2\frac{\varphi}{2}\cos^2\vartheta\right)\tilde{r} + \sin^4\frac{\varphi}{2}\cos^2\vartheta \Big\} \end{aligned} \tag{14}$$

The function f' in (14) is shown for $\varphi = 1$ in Fig. 1.

For the derivatives of b in (4) one finds in Boyer-Lindquist coordinates

$$b'_r = \frac{a'_\vartheta f'^2}{((r-m)^2 - m^2\cos^2\varphi)\sin\vartheta} \tag{15}$$

and

$$b'_\vartheta = -\frac{a'_r f'^2}{\sin\vartheta}. \tag{16}$$

Here and in the following the index in b'_r denotes the partial derivative with respect to the coordinate, here r. Integrating we find

$$b' = \frac{\sin\frac{\varphi}{2}\cos\frac{\varphi}{2}\cos\vartheta(\tilde{r} - 1)^2\left(\tan^2\frac{\varphi}{2}\cos^2\vartheta - 2\tilde{r} - 1\right)}{\tilde{r}^2 + \tan^2\frac{\varphi}{2}\cos^2\vartheta}. \tag{17}$$

Obviously an integration constant was chosen such that b' has a zero of second order at the horizon. For $r \to \infty$,

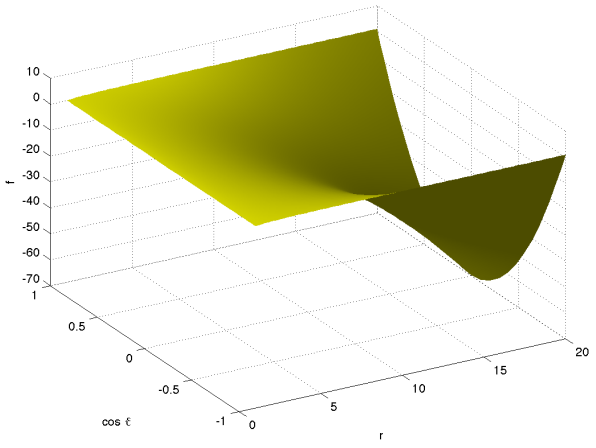

FIG. 1: Real part of the Ernst potential for the Kerr solution in coordinates corotating with the horizon (13) for $\varphi = 1$.

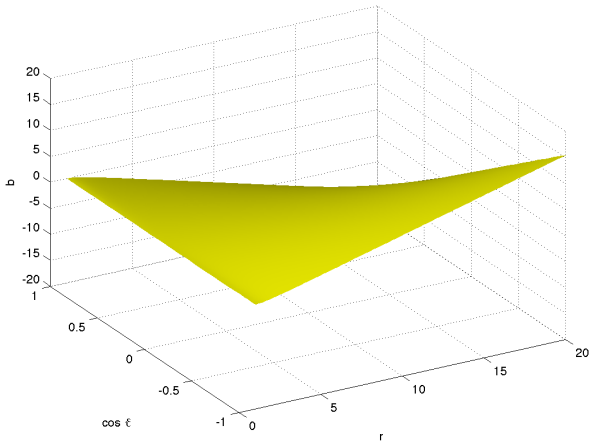

FIG. 2: Imaginary part of the Ernst potential for the Kerr solution in coordinates corotating with the horizon (17) for $\varphi = 1$.

it is proportional to $r\cos\vartheta$. It is a smooth function for all $\tilde{r} > 1$. The function is shown for $\varphi = 1$ in Fig. 2.

The remaining metric functions of h are changed by multiplication with a factor f'/f. It is obvious that $f' = a'f' = 0$ on the horizon. For large values of $r\sin\theta$, the norm f' of the Killing vector becomes negative at the light cylinder. All non-vanishing components of h except $h'_{\phi\phi} = h_{\phi\phi}$ will vanish there as f'. The function b' is as expected odd in Ω and ζ and grows linearly in ζ for $r \to \infty$. The functions $a'f'$ and f' grow as ρ^2. These kinematic contributions due to the asymptotically rotating coordinate system will be also present in the case with a helical Killing vector. For completeness we note the asymptotic behavior of the metric functions for the Kerr solution (which also holds for general asymptotically flat spacetimes) in Boyer-Lindquist coordinates,

$$\begin{aligned} f &= 1 - \frac{2m}{r} + 0(1/r^3), \\ b &= -2m^2 \sin\phi \frac{\cos\vartheta}{r^2}(1 + 0(1/r^2)), \\ a &= 2m^2 \sin\phi \frac{\sin^2\vartheta}{r}(1 + 0(1/r)), . \end{aligned} \tag{18}$$

This implies in corotating coordinates

$$f' = \left(1 - \frac{1}{\tilde{r}} - \frac{\tan^2\frac{\varphi}{2}\cos^2\vartheta}{\tilde{r}^2}\right)\left\{-\sin^2\frac{\varphi}{2}\cos^2\frac{\varphi}{2}\sin^2\vartheta(\tilde{r}^2 + \tilde{r}) + 1 - \sin^2\frac{\varphi}{2}\sin^2\vartheta - \sin^4\frac{\varphi}{2}\sin^2\vartheta\cos^2\vartheta + 0(1/\tilde{r})\right\}, \tag{19}$$

and

$$b' = -2\sin\frac{\varphi}{2}\cos\frac{\varphi}{2}\tilde{r}\cos\vartheta\left(1 - \frac{1}{2\tilde{r}}(3 + \tan^2\frac{\varphi}{2}\cos^2\vartheta) + 0(1/\tilde{r}^2))\right), \tag{20}$$

up to some irrelevant constant. Note that $m^2\sin\phi$ is just the angular momentum. If one replaces this quantity by J, one gets the behavior in the general case.

Note that the Ernst potential for the Kerr solution is often given in so called Weyl coordinates since it takes a particularly simple form in these coordinates. But in Weyl coordinates, the metric functions are not regular

at the horizon (they have a cusp like behavior where the axis intersects the horizon). Since the spectral methods we apply in this paper for the numerical solution of the Ernst equation are best adapted to analytic functions, we do not use this form of the coordinates here.

IV. ERNST EQUATION IN COROTATING COORDINATES AND KOMAR INTEGRAL

In this section we formulate the Ernst equation in Boyer-Lindquist coordinates corotating with the horizon. This equation will be solved numerically in the following sections. At some outer radius we impose the exact Kerr solution in rotating coordinates as a boundary condition. At the horizon, the vanishing of the norm of the Killing vector will be imposed. It will be argued that these two boundary conditions do not specify the solution uniquely due to a degree of freedom at the horizon (the order of the vanishing there can be essentially arbitrary which corresponds to a freedom of choosing the radial coordinate). Thus we use the Komar integral to ensure that the mass computed via the Komar integral at the horizon coincides with the ADM mass. This uniquely specifies the solution to the Ernst equation.

In the corotating coordinates introduced in the previous section, the determinant of h does not vanish at the horizon. The Ernst equation reads

$$f\left(\mathcal{E}_{rr}+\frac{1}{(r-m)^2-m^2\cos^2\varphi}\left(2(r-m)\mathcal{E}_r+\mathcal{E}_{\vartheta\vartheta}+\cot\vartheta\mathcal{E}_\vartheta\right)\right)=\mathcal{E}_r^2+\frac{\mathcal{E}_\vartheta^2}{(r-m)^2-m^2\cos^2\varphi}. \tag{21}$$

Rescaling the coordinates in a way that the radius of the horizon is equal to 1, $\tilde{r}=r/(2m\cos^2\frac{\varphi}{2})$, we get

$$f\left(\mathcal{E}_{\tilde{r}\tilde{r}}+\frac{1}{(\tilde{r}-1)(\tilde{r}-\tan^2\frac{\varphi}{2})}\left(\left(2\tilde{r}-\frac{1}{\cos^2\frac{\varphi}{2}}\right)\mathcal{E}_{\tilde{r}}+\mathcal{E}_{\vartheta\vartheta}+\cot\vartheta\mathcal{E}_\vartheta\right)\right)=\mathcal{E}_{\tilde{r}}^2+\frac{\mathcal{E}_\vartheta^2}{(\tilde{r}-1)(\tilde{r}-\tan^2\frac{\varphi}{2})}. \tag{22}$$

Since the real part of the Ernst potential vanishes for $\tilde{r}=1$ as $\tilde{r}-1$, the left-hand and the right-hand side of the equation are well-behaved at the horizon. Note that the extreme Kerr solution for $\varphi=\pi/2$ corresponds to a higher order singularity of the equation since $\tan(\varphi/2)=1$ in this case. This is the reason why it is numerically challenging to reach the extreme Kerr solution in this setting.

The idea is to solve the Ernst equation for the Kerr solution with boundary data at the horizon and at some finite outer radius. The problem with this approach is that the horizon is a singular surface of the Ernst equation, and that a regularity condition at the horizon does not uniquely specify the solution. This can be seen best at the example of the Schwarzschild solution, i.e., Kerr for $\varphi=0$. In this case one gets for the Ernst equation ($b=0$, no ϑ dependence)

$$(\ln f)_{rr}+\frac{2r-1}{r(r-1)}(\ln f)_r=0.$$

This equation has the general solution

$$f=c_1\left(\frac{r-1}{r}\right)^{c_2}, \tag{23}$$

where c_1, c_2 are constants. The constant c_1 will be fixed at infinity or the outer boundary condition, but it can be seen that the condition $f=0$ will not fix c_2 which does not have to be integer. Thus the solution is not uniquely specified by the above conditions. This is also the case for $\varphi\neq 0$. The Ernst potential is invariant under multiplication by a real constant. This freedom is fixed by the outer boundary condition. Looking for a formal solution to the Ernst equation in terms of a power series in $r-1$ near the horizon, $f=f_0(\vartheta)(r-1)^{n_f}+\ldots$, $b=b_0(\vartheta)(r-1)^{n_b}+\ldots$, we find for all $n_b>n_f$

$$n_b=2n_f, \tag{24}$$

whereas $n_f\in\mathbb{R}$ with $n_f>1/2$ and f_0, b_0 are free. This corresponds to a freedom in the choice of the radial coordinate, $\tilde{r}-1\mapsto(\tilde{r}-1)^c$ with c an arbitrary positive constant. Thus one has to formulate the boundary value problem in a way that $n_f=1$ is enforced in order to get the Kerr solution in the wanted form.

To a certain extent, the above non-uniqueness at the horizon is addressed by using dependent variables of the form $f=(\tilde{r}-1)F$ and $b=(\tilde{r}-1)^2B$. If F and B are finite at the horizon, the minimal order of the vanishing of the Ernst potential there is at least assured. With $x=\cos\vartheta$, the Ernst equation takes in this case the form

$$F\left\{(\tilde r-1)(\tilde r-\tan^2(\varphi/2))F_{\tilde r\tilde r}+(2\tilde r-1-\tan^2(\varphi/2))F_{\tilde r}+F+(1-x^2)F_{xx}-2xF_x\right\}-$$
$$(\tilde r-1)(\tilde r-\tan^2(\varphi/2))(F_{\tilde r}^2-((\tilde r-1)B_{\tilde r}+2B)^2)-(1-x^{2)}(F_x^2-(\tilde r-1)^2B_x^2) \;=\; 0, \tag{25}$$

and

$$F\left\{(\tilde r-1)(\tilde r-\tan^2(\varphi/2))B_{\tilde r\tilde r}+(4\tilde r-1-3\tan^2(\varphi/2))B_{\tilde r}+2B+(1-x^2)B_{xx}-2xB_x\right\}-$$
$$2(\tilde r-\tan^2(\varphi/2))F_{\tilde r}((\tilde r-1)B_{\tilde r}+2B)-2(1-x^2)F_xB_x \;=\; 0. \tag{26}$$

This is the form of the Ernst equation to be solved in the following sections numerically.

It turns out that this form of the equations still does not have the Kerr solution as the unique solution. Therefore we consider in the following the Komar integral associated to the Killing vector with components ξ^k

$$\int_0^{2\pi}\int_0^{\pi} g_{ik,1}g^{i0}g^{11}\sqrt{-g}d\vartheta d\varphi. \tag{27}$$

With

$$g^{11}\sqrt{-g}=(\tilde r-1)(\tilde r-\tan^2(\varphi/2))\sin\vartheta=\frac{h_{33}}{\sin\vartheta} \tag{28}$$

and

$$g^{00}=-\frac{1}{f}+\frac{fa^2}{h_{33}},\quad g^{03}=-\frac{af}{h_{33}}, \tag{29}$$

(this relation also holds in the rotating coordinate system) one gets for the Killing vector ∂_t

$$\begin{aligned} g_{ik,1}g^{ik} &= g_{03,r}g^{03}+g_{00,r}g^{00}=(\ln f)_r+\frac{aa_rf^2}{h_{33}}\\ &= (\ln f)_r-\frac{ab_\vartheta\sin\vartheta}{h_{33}}. \end{aligned} \tag{30}$$

At the horizon one has

$$\begin{aligned} f&=-\frac{\tan^2(\varphi/2)\sin^2\vartheta}{1+\tan^2(\varphi/2)\cos^2\vartheta}\\ a&=-2m\cot(\varphi/2)\\ f_r&=\frac{1}{2m\cos^4(\varphi/2)}\frac{1-\tan^2(\varphi/2)\cos^2\vartheta}{(1+\tan^2(\varphi/2)\cos^2\vartheta)^2}\\ a_r&=-\frac{1-\tan^2(\varphi/2)\cos^2\vartheta}{\sin^2(\varphi/2)\tan(\varphi/2)\sin^2\vartheta}. \end{aligned} \tag{31}$$

Thus one gets for the Komar mass the well known value

$$\frac{4\pi m}{\cos^2(\varphi/2)}\int_0^{\pi}\frac{1-\tan^2(\varphi/2)\cos^2\vartheta}{(1+\tan^2(\varphi/2)\cos^2\vartheta)^2}\sin\vartheta d\vartheta=8\pi m.$$

There is a second Killing vector in the Kerr metric, ∂_ϕ, for which the Komar integrand reads

$$(g_{03,r}g^{00}+g_{33,r}g^{03})\sqrt{-g}g^{11},$$

which at the horizon takes the form

$$\frac{a}{\sin\vartheta}(a_raf^2-h_{33,r})=4m^2\cot(\varphi/2)\sin\vartheta\left(\frac{1}{\cos^2(\varphi/2)}\frac{1-\tan^2(\varphi/2)\cos^2\vartheta}{(1+\tan^2(\varphi/2)\cos^2\vartheta)^2}+1-2\cos^2(\varphi/2)\right).$$

Integrating we find $16\pi m^2\sin\varphi=8\pi J$.

The Komar mass can be also computed in corotating coordinates. However there one has that $a'f'$ vanishes as f' at the horizon, see (14). In this case the integrand of the Komar mass reads at the horizon $-(1-\tan^2(\varphi/2))\sin\vartheta$, i.e., it does not contain information on the function F at the horizon. We get

$$4\pi m\cos^2(\varphi/2)(1-\tan^2(\varphi/2))\int_{-1}^{1}dx=8\pi(m+\Omega J).$$

Thus it is not useful to assure a non-vanishing of F at the horizon by imposing the value $8\pi(m+\Omega J)$ for the Komar integral in numerical computations. But it will allow in the case of binary black holes with a helical Killing vector to relate the values computed at the horizon to (asymptotically defined) multipoles of an asymptotically flat spacetime imposed at the outer computational boundary.

The Komar integral for the Killing vector ∂_ϕ reads

$$2\pi \int_0^\pi \left(a_r(h_{33}+a^2f^2)+h_{33}a(2(\ln f)_r-(\ln h_{33})_r)\right)\frac{d\vartheta}{\sin\vartheta}. \tag{32}$$

On the horizon the integrand reduces to $2m\cos^2(\varphi/2)a(R,\vartheta)(1-\tan^2(\varphi/2))\sin\vartheta$. Since at the horizon

$$a' = \frac{2m}{\sin(\varphi/2)\cos^3(\varphi/2)(1-\tan^2(\varphi/2))}\times \frac{1-\tan^2(\varphi/2)\cos^2\vartheta}{(1+\tan^2(\varphi/2)\cos^2\vartheta)^2}-2m\cot(\varphi/2),$$

we get for the Komar integral as before $8\pi J$. This condition will be imposed in the numerical solution of the Ernst equation.

To compute this integral, the function a has to be known, and this implies that a constant in b is fixed on the horizon. The function a can be computed from (16),

$$a_{\tilde r} = -\frac{B_\vartheta}{F^2}2m\cos^2(\varphi/2)\sin\vartheta \tag{33}$$

and from (15)

$$a_\vartheta = -\frac{(\tilde r-1)B_{\tilde r}+2B}{F^2}2m\cos^2(\varphi/2)(\tilde r-\tan^2(\varphi/2)\sin\vartheta. \tag{34}$$

V. NUMERICAL APPROACHES TO THE ERNST EQUATION

In this section we outline the numerical approaches to solve the Ernst equation in the form (25) and (26). To approximate derivatives, we use a pseudospectral approach in $\tilde r$ and x based on discretizing both coordinates. The resulting system of finite dimension for the discretized F and B is then solved with a Newton-Armijo iteration.

A. Polynomial interpolation and differentiation matrices

To solve the Ernst equation, we need to approximate numerically the derivative of a function $\mathcal{F}:[-1,1]\mapsto\mathbb{C}$. To this end we use polynomial interpolation as detailed for instance in [50]. We introduce on $[-1,1]$, the $N+1$ *Chebyshev collocation points*

$$l_j=\cos\left(\frac{j\pi}{N}\right),\quad j=0,\dots,N, \tag{35}$$

where N is some natural number. The Lagrange polynomial $p(l)$ of order N satisfying the relations $p(l_j)=\mathcal{F}(l_j)$, $j=0,\dots,N$ is then constructed. The derivative of $\mathcal{F}$ at the collocation points l_j is approximated via the derivative of this polynomial,

$$\mathcal{F}'(l_j)\approx p'(l_j)=:\sum_{k=0}^N D_{jk}\mathcal{F}(l_k),$$

where D is a *differentiation matrix*. The matrices D for Chebyshev collocation points are given in [50], a Matlab code to generate them can be found at [51]. Second derivatives of the function $\mathcal{F}$ will be approximated by $D^2\mathrm{F}$, where $\mathrm{F}_j=\mathcal{F}(l_j)$, $j=0,\dots,N$. This method is known to show *spectral convergence* for analytic functions, i.e., an exponential decrease of the numerical error with N.

This pseudo-spectral approach is equivalent to an approximation of the function $\mathcal{F}$ by a (truncated) series of Chebyshev polynomials $T_n(l)$, $n=0,\dots,N$, where

$$T_n(l)=\cos(n\arccos(l)). \tag{36}$$

A *Chebyshev collocation method* consists in approximating $\mathcal{F}$ via $\sum_{n=0}^N c_nT_n(l)$, where the *spectral coefficients* c_n are given by,

$$\mathcal{F}(l_j)=\sum_{n=0}^N c_nT_n(l_j),\quad j=0,\dots,N. \tag{37}$$

Note that because of (36), the coefficients c_n in (37) can be computed via a *fast cosine transformation* (fct) which is closely related to the *fast Fourier transform* (fft), see [50]. Since the fct is in contrast to the fft not a precompiled command in Matlab being used here, it is considerably slower than the latter. Thus we apply here the pseudospectral approach in computations. But the fct allows to control the resolution in terms of the Chebyshev coefficients: as for Fourier coefficients of real analytic functions, it is known that Chebyshev coefficients of such functions decrease exponentially with n. This allows to control that the computed functions have the expected analyticity properties. In addition it permits to control the resolution of the solution in terms of Chebyshev polynomials: if the Chebyshev coefficients decrease to machine precision (here 10^{-16}, in practice limited to roughly 10^{-14} because of unavoidable rounding errors), maximal resolution with this approach has been reached.

For the Ernst equation, we discretize $r\in[1,R]$, where R is the radius of the outer boundary, via $r_j=R(1+l_j)/2+(1-l_j)/2$, $j=0,1,\dots,N_r$ with the l_j from (35). Similarly we discretize the coordinate $x=\cos\vartheta$. Since the Kerr solution is axisymmetric, it is sufficient to consider $\theta\in[0,\pi/2]$. Thus we can write $x_j=(1+l_j)/2$ $j=0,1,\dots,N_\vartheta$ with the l_j from (35). For the Ernst potential of the Kerr solution (13) and (17) with $\varphi=1$ we get the Chebyshev coefficients shown in Fig. 3. It can be seen that the coefficients decrease to machine precision with $N_r=30$ and $N_\vartheta=20$.

B. Newton-Armijo iteration

The discretisation introduced in the previous section gives matrices with components $F(\tilde r_j,x_k)$, $B(\tilde r_j,x_k)$, $j=0,\dots,N_r$, $k=0,\dots,N_\vartheta$. These are combined to a vector G of length $2(N_r+1)(N_\vartheta+1)$. This discretisation implies

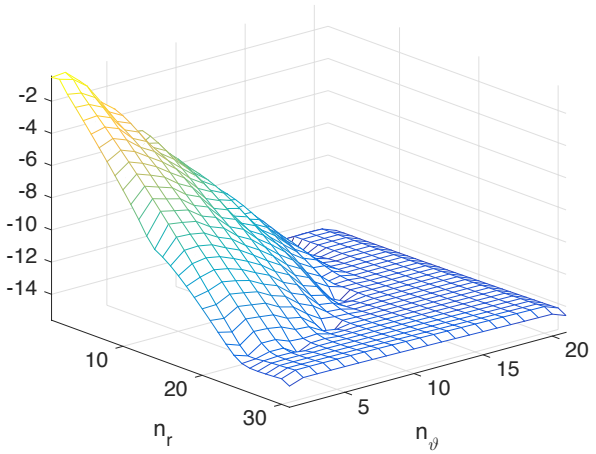

FIG. 3: Logarithm of the Chebyshev coefficients of the Ernst potential of the Kerr solution in rotating coordinates for $\varphi = 1$.

that the equations (13) and (17) are discretized in the same way. The discretized equations can be combined to a system of $2(N_r+1)(N_\vartheta+1)$ nonlinear equations of the form $\mathcal{G}(\mathrm{G}) = 0$.

This system of equations will be solved iteratively with a Newton-Armijo method giving iterate $n+1$ in dependence of iterate n,

$$\mathrm{G}_{n+1} = \mathrm{G}_n - \lambda \mathrm{Jac}^{-1}\mathcal{G}(\mathrm{G}_n), \tag{38}$$

where Jac is the Jacobian of $\mathcal{G}$ with respect to G taken for $\mathrm{G} = \mathrm{G}_n$, and where $0 < \lambda \leq 1$ is a parameter (to be discussed below) equal to 1 in the standard Newton iteration. Note that the Jacobian is a matrix of order $2(N_r+1)(N_\vartheta+1) \times 2(N_r+1)(N_\vartheta+1)$. It is known that the standard Newton iteration ($\lambda = 1$) converges quadratically. But the convergence is local, i.e., the initial iterate G_n has to be close to the exact solution to ensure convergence, see for instance the discussion in [52] and references therein.

If the initial iterate G_0 is not close enough to the solution, the standard Newton iteration fails in general to converge. A simple approach is to use some *relaxation* in the iteration, i.e., choose a value of $\lambda < 1$. This can restore convergence, but the quadratic convergence will be lost. Whereas this could be acceptable in the two-dimensional setting studied here, it certainly will not be in the three-dimensional problem for which this is a test case. But as will be discussed in the following section, even here one might be forced to use prohibitively small values of λ to avoid divergence. Therefore we apply an Armijo approach, i.e., a dynamical adjustment of the value of λ.

For each G_n in the iteration, the norm $\mathcal{N}_n := ||\mathcal{G}(\mathrm{G}_n)||_\infty$ is computed. If $\mathcal{N}_{n+1} < \epsilon$, where ϵ is the prescribed aimed at accuracy (in our case typically 10^{-10} or smaller) the iteration is stopped. If this is not the case, it is checked whether $\mathcal{N}_{n+1} < (1-\alpha\lambda)\mathcal{N}_n$. Here α is some constant which is chosen to be 10^{-4}. If the condition is met, the new iterate G_{n+1} is computed via (38) without changing the current value of λ.

If this is not the case, i.e., if the new iterate would give a worse (up to a factor $\alpha\lambda$ which can be freely chosen) solution to the equation $\mathcal{G}(\mathrm{G}) = 0$ than the previous one, a *line search* is performed: first the value of λ is halved to give a $\tilde{\lambda}$, and the corresponding value of $\mathcal{N}_l := ||\mathcal{G}(\mathrm{G}^l_{n+1})||_\infty$ is computed, where G^l_{n+1} is the G_{n+1} of (38) with the current value of λ. If this norm is smaller than $(1-\alpha\lambda)\mathcal{N}_n$, the new value is determined by a fitting to a quadratic model: the interpolation polynomial passing through the three values of the norms $\mathcal{N}_n$ for $\lambda = 0$, $\mathcal{N}_{n+1}$ for $\lambda = \lambda_o = 1$ and $\mathcal{N}_l$ for $\lambda = \tilde{\lambda}$ reads

$$p(\lambda) = \frac{(\lambda-\lambda_o)(\lambda-\tilde{\lambda})}{\lambda_o\tilde{\lambda}}\mathcal{N}_n + \frac{(\lambda-\lambda_o)\lambda}{(\tilde{\lambda}-\lambda_o)\tilde{\lambda}}\mathcal{N}_l + \frac{\lambda(\lambda-\tilde{\lambda})}{\lambda_o(\lambda_o-\tilde{\lambda})}\mathcal{N}_{n+1}.$$

The minimum value λ_m of this polynomial is taken as the new $\tilde{\lambda}$ unless it is smaller than $\lambda/10$ (in this case $\lambda/10$ is taken) or larger than $\lambda/2$ (in this case $\lambda/2$ is taken). If the condition $\mathcal{N}_l < (1-\alpha\tilde{\lambda})\mathcal{N}_n$ is still not met, the above approach is iterated with the new $\tilde{\lambda}$ and λ_o replaced by the old value of $\tilde{\lambda}$. The line search is stopped if the current value of $\tilde{\lambda}$ is smaller than 10^{-2}.

The next step of the Newton iteration is then started again with $\lambda = 1$. For details of the approach, the reader is referred to [52]. The method considerably generalizes the admissible choices for the initial iterate to achieve convergence of the Newton iteration. But obviously the closer this initial iterate is to the wanted the solution, the more rapid will be the convergence.

C. Boundary values and Komar integral

At the boundaries of the computational domain, it might be necessary to impose boundary conditions in order to avoid a degenerate Jacobian in (38). On the axis $\vartheta = \pi/2$ and at the horizon $\tilde{r} = 1$, this is not necessary since the equations (25) and (26) are singular there. Thus the condition of regularity determines the solution there, and instead of a boundary condition, just the PDE can be imposed.

The situation is different at the outer boundary $r = R$ and in the equatorial plane $\vartheta = 0$ where boundary conditions have to be enforced. At the former, just the exact Kerr solution in corotating coordinates (13) and (17) will be imposed. Alternatively the asymptotic solution (19) and (20) could be prescribed as will be done in the binary case. In the equatorial plane, we use just the equatorial symmetry of the solution which implies $F_\vartheta(\tilde{r}, 0) = b(\tilde{r}, 0) = 0$.

The conditions at the outer boundary and in the equatorial plane will be implemented via Lanczos τ-method [53]. The idea is to eliminate parts of the equation $\mathrm{Jac}(\mathrm{G}_{n+1} - \mathrm{G}_n) + \mathcal{G}(\mathrm{G}_n) = 0$ and to replace them with

the boundary conditions. Thus we replace the equations corresponding to $\tilde{r} = R$ by the Kerr solution there, and the equations corresponding to the equatorial plane by the symmetry conditions on the Ernst potential. The derivative with respect to x is approximated as all x derivatives with the corresponding differentiation matrix. It is known, see e.g. [50], that the τ method does not implement the boundary conditions exactly, but with the same spectral accuracy as the solution of the PDE is approximated.

In a similar way the Komar integral (32) is imposed. To determine the integrand at the horizon, we numerically integrate (34) to determine the function a. This is done by inverting the matrix D_x (the differentiation matrix corresponding to the coordinate x) with a vanishing boundary condition implemented at the horizon via a τ-method. The integral over the horizon is then computed with the *Clenshaw-Curtis method*: as already mentioned, the polynomial interpolation on Chebyshev collocation points is equivalent to a Chebyshev collocation method (37). Thus if an integrand is expanded in terms of Chebyshev polynomials,

$$\int_{-1}^{1} \mathcal{F}(l)dl \approx \sum_{n=0}^{N} c_n \int_{-1}^{1} T_n(l)dl = \sum_{n=0}^{N} w_n \mathcal{F}(l_n)$$

(the last step following from the collocation method (37) relating c_n and $\mathcal{F}(l_n)$) where the w_n, $n = 0, \ldots, N$ are some known weights (see [51] for a Matlab code to generate them). The Clenshaw-Curtis scheme is also a spectral method.

The condition that the Komar integral is equal to $8\pi J$ is again imposed via a τ-method as above. But this time an equation has to be replaced in (38) which is not redundant as before. We generally take the equation corresponding to (26) on the intersection of the horizon and the axis or the intersection of horizon and equatorial place. Thus the Komar integral will be implemented in the iteration in the same way as the boundary conditions.

VI. EXAMPLES

In this section, the numerical approach detailed in the previous section will be tested for various initial iterates for various values of the parameter φ. Generally the iteration converges more rapidly the smaller φ is, i.e., the farther the solution is from the extreme Kerr solution.

In this section we always choose the outer radius $R = 3$. In Fig. 4, it can be seen that the light cylinder will be for values of φ larger than 0.5 in the computational zone. Convergence of the scheme in this case will indicate that the light cylinder does not pose an insurmountable problem for the iteration.

Throughout this section we work with $N_r = 31$ and $N_\vartheta = 20$ collocation points, numbers which ensure the necessary resolution as shown by Fig. 3: the Chebyshev coefficients decrease to machine precision for $\varphi \leq 1$.

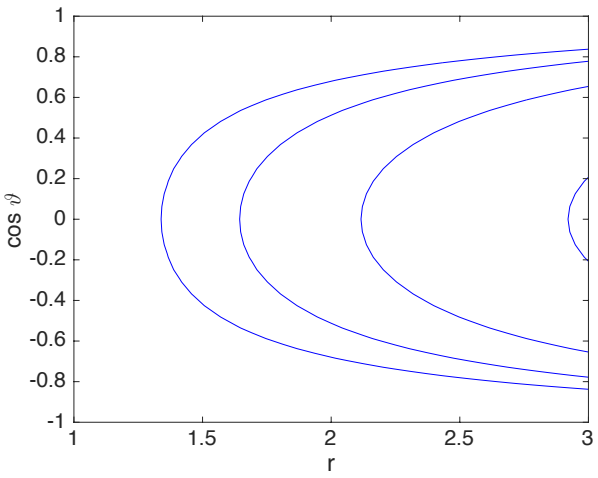

FIG. 4: Light cylinders of the Kerr solution (13) in corotating coordinates for the values of $\varphi = 0.6, 0.8, 1.0, 1.2$ from right to left.

Since we impose the Komar integral in order to obtain a unique solution at the horizon as discussed before, the condition for the Komar integral replaces one of the equations in (38). This procedure eventually leads generically to a unique solution (for special values of the parameters, there can be still other solutions to the Ernst equation satisfying the boundary conditions), but it can destabilize the iteration if the initial iterate is too far from the wanted solution. This is also the reason why we do not present a study of the dependence on the parameters N_r and N_ϑ. For smaller values of these, the iteration will not converge because of the imposed Komar integral replacing one of the equations. And without this integral, the solution to the Ernst equation will not be unique.

We first consider several initial iterates for the case $\varphi = 1$ for which according to Fig. 4 the light cylinder extends through most of the computational domain. This is already a fast spinning black hole and thus provides a good test of the scheme. As the first initial iterate we take a factor λ times the exact Kerr solution. It can be seen in Table I that for both $\lambda = 0.9$ and $\lambda = 1.1$ the iteration converges without any line search to the order 10^{-12} (the code is stopped as soon as the residual drops below 10^{-11}). The L^∞ norm of the difference between numerical and exact solution is in this case of the order of 10^{-12}. A similar behavior is observed if the exact Kerr solution plus 0.1 times a Gaussian in $\tilde{r}$ is taken as initial iterate. If we take as the initial iterate the exact Kerr solution for $\varphi = 0.9$, the iteration converges after 5 iterations to the order of 10^{-12}. This appears to be the optimal accuracy reachable with the approach. The above examples show that the iteration is stable and converges rapidly for various initial iterates to an accuracy of better than 10^{-11} both as a residual to the numerically implemented equations and compared to the exact solution.

initial iterate	iterations	$\|\|u - u_{Kerr}\|\|_\infty$
$u_{Kerr}(\varphi = 0.9)$	7	$1.9 * 10^{-12}$
$1.1u_{Kerr}(\varphi = 1)$	5	$1.7 * 10^{-12}$
$u_{Kerr}(\varphi = 1) + 0.1\exp(-\tilde{r}^2)$	6	$1.7 * 10^{-12}$
$0.9u_{Kerr}(\varphi = 1)$	5	$2.1 * 10^{-12}$

TABLE I: A table of the convergence of the iteration scheme for $\varphi = 1$ and various initial iterates.

initial iterate	iterations	$\|\|u - u_{Kerr}\|\|_\infty$
$0.9u_{Kerr}(\varphi = 1.5)$	14	$2.0 * 10^{-10}$
$1.1u_{Kerr}(\varphi = 1.5)$	8	$2.1 * 10^{-10}$
$u_{Kerr}(\varphi = 1.495)$	10	$2.1 * 10^{-10}$
$u_{Kerr}(\varphi = 1.5) + 0.01\exp(-\tilde{r}^2)$	6	$2.0 * 10^{-10}$

TABLE II: A table of the convergence of the iteration scheme for $\varphi = 1.5$ and various initial iterates.

φ	iterations	$\|\|u - u_{Kerr}\|\|_\infty$
0.1	6	$4.8 * 10^{-12}$
0.2	9	$3.3 * 10^{-12}$
0.3	8	$3.8 * 10^{-12}$
0.4	30	$2.1 * 10^{-12}$
0.5	9	$2.5 * 10^{-11}$
0.6^*	24	$2.4 * 10^{-12}$
0.7^*	9	$2.5 * 10^{-12}$
0.8	6	$1.3 * 10^{-11}$
0.9	6	$1.3 * 10^{-12}$
1	7	$1.9 * 10^{-12}$

TABLE III: A table with the convergence of the iterative solution of the Ernst equation for various values of φ. The initial iterate is always the exact Kerr solution for $\varphi - 0.1$ except for the cases marked with a star: for $\varphi = 0.6$, the iteration is started with the value 0.51, for $\varphi = 0.7$ with $\varphi = 0.66$.

The used form of the Ernst equation does not allow to treat the extreme Kerr solution in this way. The reason for this is that the horizon no longer corresponds to a regular singularity of the equations in this case, and that the light cylinder touches the horizon. It would be necessary to address this case explicitly, but this is not the goal here. However, it is interesting to note that one gets rather close to the extreme Kerr solution. One has just to find better initial iterates in this case to get convergence. For $\varphi = 1.5$, we get for an initial iterate of a factor λ times the exact solution again rapid convergence, see Table II. Note that in this case the exact location of the light cylinder is the correct one of the wanted Kerr solution. The situation is similar for an initial iterate of the exact solution plus a small Gaussian in $\tilde{r}$. But only for a Gaussian of maximum 0.01, not for 0.1 as before in Table I. There is also no convergence if the exact Kerr solution with $\varphi = 1.4$ is taken, one has to be as close as $\varphi = 1.495$. In all cases the L^∞ norm of the difference between numerical and exact solution is of the order of 10^{-10}.

The above results indicate that it might be possible to start the iteration close to the static Schwarzschild solution and use the found numerical solution for a given value of φ as initial iterates for larger values of φ. This would allow to increase the angular momentum of the black hole in the iterations. The steps have to be smaller the closer one is to the extreme black hole. Problems in this approach are obviously related to the location of the light cylinder. Whereas an initial iterate of the form of the exact Kerr solution multiplied by some factor leads to rapid convergence, this is not the case for an initial iterate with a clearly different form of the light cylinder. This is not surprising since the latter corresponds to a singularity of the Ernst equation. In fact in can be seen in Table III that the iteration converges rapidly up to values of $\varphi = 0.5$ if the initial iterate is the Kerr solution with $\varphi - 0.1$. It is clear from Fig. 4 that in these cases, there is no light cylinder in the computational domain. Convergence problems appear for $\varphi = 0.6$ and $\varphi = 0.7$ for which the light cylinder appears very close to the outer computational boundary $R = 3$. Here the initial iterate must be close to the final solution, i.e., the light cylinder should be close to its exact location. For larger values of φ, the light cylinder is not only localized close to the boundary as can be seen in Fig. 4, and the iteration converges again rapidly. Thus it appears that special care has to be taken in the choice of the initial iterate if the light cylinder appears only close to the outer boundary of the computational domain, or if it is close to the horizon as in almost extreme black holes.

VII. OUTLOOK

In the previous section we have shown that the Ernst equation in the form (25) and (26) can be solved iteratively for a Kerr black hole in a frame corotating with the horizon. The numerically challenging part is the location of the light cylinder which is a singularity for the equation. The main problems arise if the light cylinder is located close to the boundary of the computational domain or close to the horizon as in almost extreme black holes. It was shown that these difficulties could be addressed by performing line searches in the iteration.

A technical problem of the Ernst equation is the fact that the latter is homogeneous in the Ernst potential which implies that with $\mathcal{E}$ also a constant times $\mathcal{E}$ is a solution. In addition the order of the vanishing of the Ernst potential at the horizon is not uniquely fixed. Thus the asymptotic behavior of the Ernst potential together with a regularity condition at the horizon does not uniquely identify the solution. Therefore we used the Komar integral for the Killing vector ∂_ϕ to establish a unique solution.

The above results indicate that the Ernst approach should also allow a numerical solution in the case of binary black holes with a helical Killing vector. The idea is to use adapted coordinates as bispherical coordinates in which the horizons are given as constant coordinate

surfaces, for instance the approach [54]. The Einstein equations in the projection formalism will be solved with a spectral method and an Newton-Armijo approach as in the present paper on a finite computational domain. At the boundary of the computational domain, a solution to the linearized Einstein equations as in [29] or an asymptotically flat solution will be imposed as boundary conditions. This will be the subject of further work.

Acknowledgments

This work has been supported by the ANR via the program ANR-09-BLAN-0117-01 and the region of Burgundy. We thank R. Beig, J. Frauendiener, and P. Grandclément for helpful remarks and hints.

[1] B. P. Abbott et al., *Phys. Rev. Lett.* **116**, 061102 (2016).
[2] U. Sperhake, *Class. Quantum Grav.* **32** 124011 (2015).
[3] S. Detweiler, in *Frontiers in Numerical Relativity*, ed. by C.R. Evans, L.S. Finn and D.W. Hobill (CUP, Cambridge, England), 43 (1989).
[4] J. Blackburn and S. Detweiler, *Phys. Rev. D* **46**, 2318 (1992).
[5] S. Detweiler, *Phys. Rev. D*, **50**, 4929 (1994).
[6] M. Schönberg, *Phys. Rev.* **69**, 211 (1946).
[7] A. Schild, *Phys. Rev.* **131**, 2762 (1963).
[8] J. Friedman, K. Uryu and M. Shibata, *Phys. Rev. D*, **65**, 064035 (2002).
[9] E. Gourgoulhon, P. Grandclément and S. Bonazzola *Phys. Rev. D* **65**, 044020 (2002).
[10] P. Grandclément, E. Gourgoulhon and S. Bonazzola *Phys. Rev. D* **65**, 044021 (2002).
[11] Z. Andrade, C. Beetle, A. Blinov, B. Bromley, L. Burko, M. Cranor, R. Owen and R. Price, gr-qc/0310001 (2003).
[12] M. Caudill, G.B. Cook, J.D. Grigsby, and H.P. Pfeiffer Phys. Rev. D 74, 064011 (2006)
[13] K. Uryu, F. Limousin, J.L. Friedman, E. Gourgoulhon, and M. Shibata Phys. Rev. D 80, 124004 (2009)
[14] J.L. Friedman and K. Uryu Phys. Rev. D 73, 104039 (2006)
[15] N.T. Bishop, R. Gómez, L. Lehner, M. Maharaj, and J. Winicour Phys. Rev. D 72, 024002 (2005)
[16] K. Uryu, E. Gourgoulhon, and C. Markakis, Phys. Rev. D 82, 104054 (2010)
[17] S. Yoshida, B.C. Bromley, J. S. Read, K. Uryu, and J.L. Friedman, Class. Quant. Grav. 23(16) (2006)
[18] C. Beetle, B. Bromley, and R.H. Price Phys. Rev. D 74, 024013 (2006)
[19] B. Bromley, R. Owen, and R.H. Price Phys. Rev. D 71, 104017 (2005)
[20] C. Beetle, B. Bromley, N. Hernández, and R.H. Price Phys. Rev. D 76, 084016 (2007)
[21] S.R. Lau, R.H. Price, Journ. Comp. Phys. 227(2), 1126 (2007)
[22] S.R. Lau, R.H. Price, Journ. Comp. Phys. 231(22), 7695 (2012)
[23] S. Bonazzola, J.L. Jaramillo and J. Novak. Class. Quant. Grav. 24(16) (2007)
[24] A. Le Tiec, L. Blanchet, and B.F. Whiting Phys. Rev. D 85, 064039 (2012)
[25] A. Le Tiec Class. Quant. Grav. 29(21) (2012)
[26] S.E. Gralla and A. Le Tiec, Phys. Rev. D 88, 044021 (2013)
[27] G. Gibbons and J. Stewart, in *Classical general Relativity*, ed. by W. Bonnor, J. Islam and M. MacCallum (CUP, Cambridge, England), 77 (1984).
[28] A. Ashtekar and B. Xanthopoulos, *J. Math. Phys.* **19**, 2216 (1978).
[29] C. Klein, *Binary black holes with a helical Killing vector*, Phys. Rev. D, Vol. 70, 124026 (2004).
[30] J.M. Stewart, *Class. Quant. Grav.* **18**, 4983 (2001).
[31] C. Ferrari and F.G. Tricomi, *Transonic Aerodynamics* (Academic Press, New York, 1968); J.D. Cole and L.P. Cook, *Transonic Aerodynamics* (North-Holland, Amsterdam, 1986).
[32] K.O. Friedrichs, *Comm. Pure Appl. Math.* **11**, 333 (1958).
[33] P. Lax and R. Phillips, *Comm. Pure Appl. Math.* **13**, 427 (1960).
[34] C. Torre, J.Math.Phys. 44, 6223-6232(2003).
[35] C.G. Torre, J. Math. Phys. 47 073501 (2006)
[36] T.H. Otway, Jour. Geom. Phys., 58(8), 1043 (2008)
[37] T.H. Otway, Overview of EllipticHyperbolic PDE, EllipticHyperbolic Partial Differential Equations, SpringerBriefs in Mathematics (2015)
[38] T.H. Otway, The Dirichlet Problem for EllipticHyperbolic Equations of Keldysh Type, Lecture Notes in Mathematics 2043 (2011)
[39] R. Beig, J.M. Heinzle, and B.G. Schmidt Phys. Rev. Lett. 98, 121102 (2007)
[40] J. Bicák and Bernd G. Schmidt Phys. Rev. D 76, 104040 Published 27 November 2007
[41] J. Bicák, M. Scholtz , P. Tod, Relativity and Gravitation 157, Springer Proceedings in Physics 267-273 (2014)
[42] J. Ehlers, *Konstruktion und Charakterisierungen von Lösungen der Einstein'schen Gravitationsgleichungen*, Dissertation (in German), Hamburg (1957).
[43] R. Geroch, *J. Math. Phys.*, **12**, 918 (1971).
[44] D. Maison in *Lecture Notes Phys. 1-126*, **540** (2000).
[45] F. J. Ernst, *Phys. Rev*, **167**, 1175 (1968).
[46] W.J. Zakrzewski, *Low-dimensional Sigma Models* Institute of Physics Publishing, (1989).
[47] C. Klein and O. Richter, *Ernst Equation and Riemann Surfaces*, Lecture Notes in Physics Vol. 685 (Springer, Berlin, 2005).
[48] L. Armijo, *Pacific J. Math.* **16** (1966) no. 1, 1-3.
[49] D. Kramer, H. Stephani, E. Herlt and M. MacCallum, *Exact Solutions of Einstein's Field Equations*, Cambridge: CUP (1980).
[50] L.N. Trefethen, Spectral Methods in Matlab. SIAM, Philadelphia, PA (2000)
[51] www.comlab.ox.ac.uk/oucl/work/nick.trefethen
[52] C.T. Kelley, Iterative Methods for Linear and Nonlinear Equations (SIAM, Philadelphia, 1995).
[53] C. Lanczos, Trigonometric interpolation of empirical and analytic functions, J. Math. and Physics, 17, 123-199 (1938)
[54] P. Grandclément, J. Comp. Phys. 220, 3334 (2010).